

Effect of a local quantum dynamical process on the quantum state transfer and Loschmidt echo

Saikat Sur* and V. Subrahmanyam†

Department of Physics, Indian Institute of Technology, Kanpur 208016, India

(Dated: May 16, 2022)

The effect of a local instantaneous quantum dynamical process (QDP), either unitary or non-unitary, on the quantum state transfer through a unitary Hamiltonian evolution is investigated for both integrable and non-integrable dynamics. There are interference effects of the quantum state propagation and the QDP signal propagation. The state transfer fidelity is small for further sites, from the site where the information is coded, indicating a finite speed for the propagation of the quantum correlation. There is a small change in the state transfer fidelity for the case of non-unitary QDP intervening the background unitary dynamics. In the case of unitary QDP, the change is more pronounced, with a substantial increase in the fidelity for appropriate sites and times. The Loschmidt echo is investigated to track the effect of the local QDP. It is also quite sensitive to whether the background dynamics is integrable or not. For the integrable case, viz. the Heisenberg model, the Loschmidt echo falls off as a function of the time of QDP occurrence, and saturates to a value, depending on the parameter values. For the non-integrable case, viz. a kicked Harper model, it exhibits an oscillatory behaviour around a larger value. The state transfer fidelity, in this case, is quite large for further sites for short times, indicating a finite speed for the propagation of the quantum correlation cannot be defined.

I. INTRODUCTION

Quantum spin chains have been investigated, over the last few years, from the viewpoint of quantum information and communication. A quantum spin chain serves as a possible channel for the quantum state transfer[1–3]. These systems have been studied extensively, as exactly-solvable condensed matter physics systems, for studying spin ordering of novel spin states, and quantum critical behaviour.[4–6]. These studies deal with the quantum dynamics of initial many-body states through the Schrodinger time evolution[7], and the statistical mechanics of the phase transitions[4, 7].

The spin chain dynamics can be treated viewing the spin chain as a closed system, with a given initial state with a distribution of correlations. Through the time evolution the quantum correlations can be redistributed and the spin chain can exhibit a variety of multi-party quantum correlation and entanglement structures. The wide spectrum of the dynamics investigation of spin chains includes the study of magnon bound states and scattering[8, 9], spin current and relativistic density wave dynamics[10, 11], quantum correlations after a quench[12] and light-cone in entanglement spreading[13]. The effect of unitary evolution of the quantum spin chain can be viewed as, in the quantum information language, various global and local multi-qubit gate operations acting on the many-qubit system. The system will undergo a redistribution of entanglement and quantum correlations[14–18] through the unitary evolution. However, a multi-party qubit system in general can experience decoherence due to incoherent processes acting on

some qubits locally or globally, that can lead decoherence. Investigating the effect of local decohering process on the quantum correlations and the entanglement structure is difficult in general, as traditional approximation tools like the time-dependent perturbation theory are not applicable for these systems. In a simple example of local decohering process intervening the Schrodinger evolution of quantum states is investigated[19], where a the Hamiltonian unitary evolution of a many-qubit quantum state is interrupted by a local instantaneous quantum dynamical process (QDP) on a certain qubit at a certain epoch of time. The QDP can be a non-unitary decohering operation or a unitary operation different from the back ground evolution. The QDP signal, the effect of the occurrence of the process at a given time and location, and its propagation have been investigated using both conserving and non-conserving dynamics for initial states with and without entanglement for various model Hamiltonian dynamics. The signal propagation speed in general depends on the type of interaction of the qubits, the strength of the interaction, the spatial range of the interaction and the initial state.

The quantum state transfer protocol[1–3, 22] studied for the spin chains relies on the Hamiltonian evolution for a faithful communication and detection of the state from an initial qubit location to a target qubit location. The average fidelity, averaged over all possible input qubit state, of the state transfer, is a figure of merit of the protocol. The fidelity depends on the interaction parameters of the Hamiltonian, and in general it is oscillatory as a function of the time of evolution as a result of quantum interference. The state transfer fidelity can have non trivial effects due to the QDP intervention of the unitary evolution, and the fidelity can also increase if it is a unitary QDP; the detailed investigation of these effects is the main focus of this paper. The quantum

* saikatsu@iitk.ac.in

† vmani@iitk.ac.in

interference, between the quantum correlation generation and distribution due to the Hamiltonian evolution of a uncorrelated initial state and the quantum effect of the local quantum process occurring at a given qubit at a given time, can also be studied using the Loschmidt echo[20], calculated from the overlap of the time evolved multi-qubit states with and without QDP. As we will discuss below, apart from detecting the effect of the QDP, the Loschmidt echo exhibits a contrasting behaviour for integrable and non-integrable background Hamiltonian evolutions. Whereas, the state transfer fidelity gives a measure of quantum interference and correlation effects between the local qubit encoding the quantum bit information and the local qubit measuring the quantum bit information, the Loschmidt echo gives a global measure of the quantum interference between the many-qubit state evolved with a local QDP intervening at given time and location and a many-qubit state evolved without a QDP. These aspects are studied here analytically for integrable dynamics using the anisotropic Heisenberg model, where analytical solutions are available, and numerically for non-integrable dynamics using the Harper model. In Section II, we outline the quantum state transfer protocol and the computation of the transfer fidelity. We will study the effect of a local decohering process in Section III, followed by a local coherent process in Section IV, the computation of the fidelity using one and two qubit Green's functions. In Section V, the Loschmidt echo is investigated for the QDP. We will discuss a local decohering process in non-integrable systems in Section VI.

II. QUANTUM STATE TRANSFER THROUGH UNITARY DYNAMICS

Faithful and faultless transmission of quantum states between two distant locations is the main challenge for quantum communication and information processing protocols. The quantum spin chains as channels of quantum state transfer was proposed and investigated[1, 2, 22]. The spin of the electrons are basic examples of qubits, viz. two-level quantum systems, and the spin chains can be realised physically in magnetic systems. One-dimensional spin models have been studied extensively using the Heisenberg-XY or transverse-field Ising model Hamiltonians, due to their exact solvability using the Bethe ansatz technique or Jordan-Wigner fermion technique respectively. In this paper, we will be using the Heisenberg dynamics for the most part, and will study a variant of transverse-XY model in the last section.

In a standard state transfer protocol, a direct product many-qubit initial state is prepared, at time $t = 0$, with the first spin in a desired state (or the information is coded into the state of the first spin). The many-qubit state is evolved through time using the Hamiltonian Schroedinger dynamics to a final state at time t . Then the desired state is to be recovered from a certain target spin, the probability of the state transfer is mea-

sured by the fidelity, normalised to unity, computed by taking the overlap of the target state with the desired state. A large value of the state transfer fidelity for a spin at a particular location at a particular time implies the efficacy of the state transfer protocol. In this paper, we will deviate from the standard protocol, and intervene the smooth Heisenberg-XY dynamics by a local quantum dynamical process (QDP) at a given location and time, viz. an instantaneous quantum operation is carried out on the many-qubit state at a time $t = t_0$, between the coding time $t = 0$ of the quantum information at the first spin, and the recovery or readout time t of the quantum information from a different spin. In this paper the focus would be on the effect of QDP on quantum state transfer fidelities. We will see that local QDPs can decrease or increase the fidelity depending upon their locations and time. In this context we will discuss the reversibility of a quantum state due to an imperfect unitary evolution. Also, we will discuss the state transfer and the effect of local QDP with a non integrable background Hamiltonian dynamics, and investigate the signature of quantum chaos in Sec. V.

Let us consider a one-dimensional array of N qubits interacting through a nearest-neighbour exchange interaction, and a particular qubit state has to be transferred from one end to the other. The protocol encodes the information to be transferred in to the state $|\phi\rangle = \alpha|0\rangle + \beta|1\rangle$. The first qubit is initialised to this state at one end, the many qubit initial state is $|\psi(0)\rangle = |\phi 00\dots 0\rangle$, a direct product of the state $|\phi\rangle$ for the first qubit and the state $|0\rangle$ for all other qubit. The unitary time evolution will transform the many qubit state to $|\psi(t)\rangle$ using the Hamiltonian dynamics. The desired qubit $|\phi\rangle$ can spread out to other qubits during the evolution, i.e., the desired qubit state can travel to the other locations with a some speed and probability. The speed associated with such transfer is inversely related to the interaction strength between the sites. For an efficient state transfer, the target state ρ_l , is the reduced density matrix of the l 'th qubit, calculated by taking a trace over all other qubits from the many qubit state, $\rho_l = \text{tr}'|\psi(t)\rangle\langle\psi(t)|$, should be the same as the desired state $\rho_\phi = |\phi\rangle\langle\phi|$. The state transfer fidelity gives a probabilistic measure of the state transferred from one site to another and is quantified by taking overlap of the target and the desired states, given by

$$\mathcal{F}_{l,\phi} \equiv \text{Tr}\rho_\phi\rho_l = \langle\phi|\rho_l|\phi\rangle. \quad (1)$$

Now, the fidelity shown above depends on the initial state ϕ , apart from the target spin location and time, and the interaction parameters of the Hamiltonian dynamics. A figure of merit measure for the efficacy of the protocol is to average the above over all possible initial qubit states, i.e., over the surface of the Bloch sphere representing all qubit pure states.

The first exactly-solvable and integrable non trivial models of interacting quantum spins is a one-dimensional chain of spins interacting with their nearest neighbour

Heisenberg exchange interaction, known as the Heisenberg model. We will use the Pauli operator $\vec{\sigma}_i$ to represent the different components of the spin operator \vec{S}_i at i 'th site. Let us consider a one-dimensional chain of N spins interacting through the nearest-neighbour anisotropic Heisenberg model. The Hamiltonian is given by,

$$H = -J \sum_i \sigma_i^x \sigma_{i+1}^x + \sigma_i^y \sigma_{i+1}^y + \Delta \sigma_i^z \sigma_{i+1}^z. \quad (2)$$

where J is the exchange interaction strength for the nearest-neighbour spins, and Δ is the anisotropy strength. As all the three Pauli spin matrices appear in the Hamiltonian, an exchange interaction of neighbouring spin is implied in all three spin dimensions. The model exhibits ferromagnetic (antiferromagnetic) behaviour in the ground state for $\Delta > 0$ ($\Delta < 0$). The ground state and all the excited states are known, and can be found using the Bethe ansatz[6]. Let us use the basis states for the i 'th spin as $|0\rangle$ (up-spin state) and $|1\rangle$ (down-spin) states, denoting the eigenstates σ_i^z with eigenvalues $+1$ and -1 respectively. The basis states for the many-qubit system can be chosen to be the direct products of the basis states of each spin. The z-component of the total spin $\sum \sigma_i^z$ is a constant of motion, which implies that the eigenstates will have a definite number of down spins. The many-qubit basis states with l down spins can also be labeled by the locations (x_1, x_2, \dots, x_l) of the l down spins, where the set is an ordered set with $x_1 < x_2$ and so on. An eigenstate with l down spins, a l -magnon state, can be written as a superposition of the basis states as,

$$|\psi\rangle = \sum_{x_1, x_2, \dots, x_l} \psi(x_1, x_2, \dots, x_l) |x_1, x_2, \dots, x_l\rangle \quad (3)$$

where the eigenfunction $\psi(x_1, x_2, \dots, x_l)$ denotes the wave function amplitude for the corresponding basis state. The eigenfunction is given by the Bethe Ansatz[21], labeled by the set of momenta (p_1, p_2, \dots, p_l) of the down spins, which are determined by solving algebraic Bethe ansatz equations, with periodic boundary conditions. There is only one zero-magnon state $|F\rangle = |00\dots 0\rangle$, which is just a ferromagnetic ground state with all the spins polarized along one direction. It is straightforward to see that it is an eigenstate of the above Hamiltonian with energy $\epsilon_0 = -NJ$ for periodic boundary conditions (closed chain), and $\epsilon_0 = -J(N-1)$ for open boundary conditions (open chain). Starting from $|F\rangle$, one-magnon excitations can be created by turning any one of the spins, giving N localised one-magnon states, which can be labeled by the location of the down spin. One-magnon eigenstates are labeled by the momentum of the down spin, the eigenfunction is given by,

$$\begin{aligned} \psi_p^x &= \sqrt{\frac{1}{N}} e^{ipx}; p = \frac{2\pi I}{N}, \text{ for a closed chain} \\ \psi_p^x &= \sqrt{\frac{2}{N+1}} \sin(px); p = \frac{\pi I}{N+1}, \text{ for an open chain,} \end{aligned} \quad (4)$$

where the momentum p is determined by an integer $I = 1, 2, \dots, N$ for both cases. The one-magnon eigenvalue is given by $\epsilon_1(p) = \epsilon_0 - 2J \cos p$. The interaction strength J determines the hopping of the down spins to neighbouring sites, and the interaction of the two down spins is determined by Δ . The one-magnon eigen energies are independent of Δ as the states carry only one down spin. The two-magnon ($l=2$) and other eigenstates ($l \geq 2$) include both scattering states and bound states of the down spins. The eigenfunction for the two-magnon eigenstate is labeled by two momenta p_1 and p_2 , is given by

$$\psi_{p_1, p_2}^{x_1, x_2} = A(p_1, p_2) (e^{ip_1 x_1} e^{ip_2 x_2} + e^{i\theta(p_1, p_2)} e^{ip_1 x_2} e^{ip_2 x_1}), \quad (5)$$

where $A(p_1, p_2)$ is a normalisation factor. The two terms in the wave function differ by a permutation of the positions x_1 and x_2 . The phase factor $\theta(p_1, p_2)$ depends on the moment and the interaction strengths, and is given by

$$\tan \frac{\theta(p_1, p_2)}{2} = \frac{\Delta \sin[(p_1 - p_2)/2]}{\cos[(p_1 + p_2)/2] - \Delta \cos[(p_1 - p_2)/2]}. \quad (6)$$

The two momenta are determined by the Bethe ansatz equations,

$$p_1 N = 2\pi I_1 + \theta(p_1, p_2), \quad p_2 N = 2\pi I_2 - \theta(p_1, p_2), \quad (7)$$

where I_1, I_2 are any integers. The two-magnon eigenvalues are given by $\epsilon_2(p_1, p_2) = \epsilon_0 + 2(\Delta - \cos p_1) + 2(\Delta - \cos p_2)$. The detail of solving the above Bethe ansatz equations for the two-magnon scattering and bound states is discussed in the Appendix A, along with the computation of the time-dependent Green's functions.

We will see no dynamics effects if the initial state is this eigenstate of the Hamiltonian. To study the dynamics of an arbitrary initial state, we will consider a linear combination of zero-magnon, one-magnon and two-magnon states that are not eigenstates of the Hamiltonian, in conjunction with the QDP dynamics below. Let us consider a spin chain with open boundary condition and the initial state given by,

$$|\psi(0)\rangle = \alpha |00\dots 0\rangle + \beta |100\dots 0\rangle = \alpha |F\rangle + \beta |x=1\rangle, \quad (8)$$

where x denotes location of the down spin. The above state is a linear superposition of an eigenstate of the Hamiltonian with eigenvalue ϵ_0 and a one magnon state which can be written as a linear combination of one-magnon momentum eigenstates $|p\rangle$ of the Hamiltonian with eigenvalues $\epsilon_1(p)$, we have

$$|\psi(0)\rangle = \alpha |F\rangle + \beta \sum_p \psi_p(1) |p\rangle, \quad (9)$$

Now, the time evolution of the system will transport the single down spin from the first site to other sites and the state after a time t becomes,

$$|\psi(t)\rangle = \alpha e^{-i\epsilon_0 t} |F\rangle + \beta \sum_y G_1^y(t) |y\rangle, \quad (10)$$



Figure 1. The evolution of the initial state $\rho(0)$ in three steps: The state evolves to $\rho(t_0^-)$ through a unitary process using the Heisenberg Hamiltonian till $t = t_0^-$, the state become $\tilde{\rho}(t_0^+)$ through an instantaneous local QDP at $t = t_0$, and finally it evolves to $\tilde{\rho}(t)$ through the same unitary process.

where the time-dependent function $G_x^{x'}(t)$ [19] is given in terms of the wave functions defined above as,

$$G_x^{x'}(t) = \sum_p \psi_p^x \psi_p^{x'*} e^{-it\epsilon_1(p)}. \quad (11)$$

Using the one-magnon eigenfunctions, shown in Eq.4, we can express the Green's function as,

$$G_x^{x'}(t) = \frac{N}{2\pi} \int_0^\pi \psi_p^x \psi_p^{x'*} e^{-it\epsilon(p)} dp = (-i)^{(x-x')} J_{(x-x')}(2t) - (-i)^{(x+x')} J_{(x+x')}(2t), \quad (12)$$

for an open chain, and we have

$$G_x^{x'}(t) = (-i)^{(x-x')} J_{(x-x')}(2t), \quad (13)$$

for a closed chain. The reduced density matrix (RDM) of the l^{th} qubit is defined by taking trace of the whole quantum state over all qubits except the l^{th} one, as $\rho_l = Tr' \rho(t)$, where $\rho(t) = |\psi(t)\rangle\langle\psi(t)|$, is the time-evolved many-qubit state. Using the basis $|0\rangle, |1\rangle$ for the l^{th} qubit, the reduced density matrix is given by,

$$\rho_l(t) = \begin{pmatrix} 1 - x_l(t) & y_l(t) \\ y_l^*(t) & x_l(t) \end{pmatrix}, \quad (14)$$

where the elements of the RDM are time dependent functions that can be calculated from Eq.10 as,

$$x_l(t) = \langle 1 | \rho_l(t) | 1 \rangle = |\beta|^2 |G_1^l(t)|^2, \quad (15)$$

$$y_l(t) = \langle 0 | \rho_l(t) | 1 \rangle = \alpha \beta^* e^{-i\epsilon_0 t} G_1^{*l}(t).$$

The state transfer fidelity for the l^{th} site as a function of time is given by,

$$\mathcal{F}_{l,\phi}(t) = |\alpha|^2 (1 - x_l(t)) + |\beta|^2 x_l(t) + 2Re(\alpha^* \beta y_l(t)). \quad (16)$$

The quantity $\mathcal{F}_{l,\phi}(t)$ depends on the parameters α and β of the initial state. The averages over the parameters in the above equations are given as $|\alpha|^2 = |\beta|^2 = \frac{1}{2}$, $|\alpha|^2 |\beta|^2 = \frac{1}{6}$ and $|\beta|^4 = \frac{1}{3}$. Taking the average over all possible pure states on the Bloch sphere characterised by α and β the average state transfer fidelity [1] becomes,

$$\mathcal{F}_l(t) = \frac{1}{2} + \frac{1}{6} |G_1^l(t)|^2 + \frac{1}{3} Re(e^{i\epsilon_0 t} G_1^l(t)). \quad (17)$$

The state transfer fidelity $\mathcal{F}_l(t)$ with unitary dynamics is shown in Fig. 2(a) as a function of time for different

site indices. Since the function $G_1^l(t)$ is a Bessel function with time as argument it falls inversely with time and the fidelity of state transfer decreases with time for a particular site and over a large time saturates to the value 0.5. It also decreases with the increase in the distance between the first site and the decoding site l . The maximum fidelity for the site l is obtained around time $l/2$ (here, we have taken interaction strength $J = 1/2$). So, the speed of state transfer is equal to the value of interaction strength J between the spins.

III. LOCAL QUANTUM DECOHERING PROCESS

We now consider the effect of a local QDP intervening the smooth unitary dynamics, thus effect the state transfer protocol. The time evolution of a general state involves, as we have seen in the previous section, the coherent movement of the down spins, due to the unitary dynamics generated by the Heisenberg Hamiltonian we are considering. The QDP we consider below occurs instantaneously at a time $t = t_0$, operating on a certain spin, thus changing the whole many-qubit state instantaneously. That is the QDP occurs between the time $t = t_0^-$ and the time $t = t_0^+$. The dynamics is unitary for $t < t_0^-$, and again for $t > t_0^+$, and it is given by the Heisenberg Hamiltonian. The QDP can be non-unitary, which causes explicit decoherence of the many-qubit state, considered in this section, or the QDP can be another coherent quantum operation that will be discussed in the next section. First, we consider a non-unitary QDP that is a local decohering process, as an example, a projective measurement of σ_m^z which has two outcomes, corresponding projectors $P_0 = (1 + \sigma_m^z)/2$ and $P_1 = (1 - \sigma_m^z)/2$. A more general measurement operators, for example measuring an arbitrary component of $\vec{\sigma}_m$, have been considered and seen to be qualitatively similar [19]. Thus, now we have marked three qubits, at three different locations, namely, the first qubit where the initial information is coded, the l^{th} qubit where we recover the desired state transfer, and the m^{th} qubit where a local QDP occurs. We will see below the case of $l > m$, in which both the desired state from the first spin and the effect of QDP will have to travel in the same direction to reach the recovery site, and the case of $m > l$ in which the two effects travel to the recovery site from opposite directions. There will be interesting quantum interferences effects, particularly

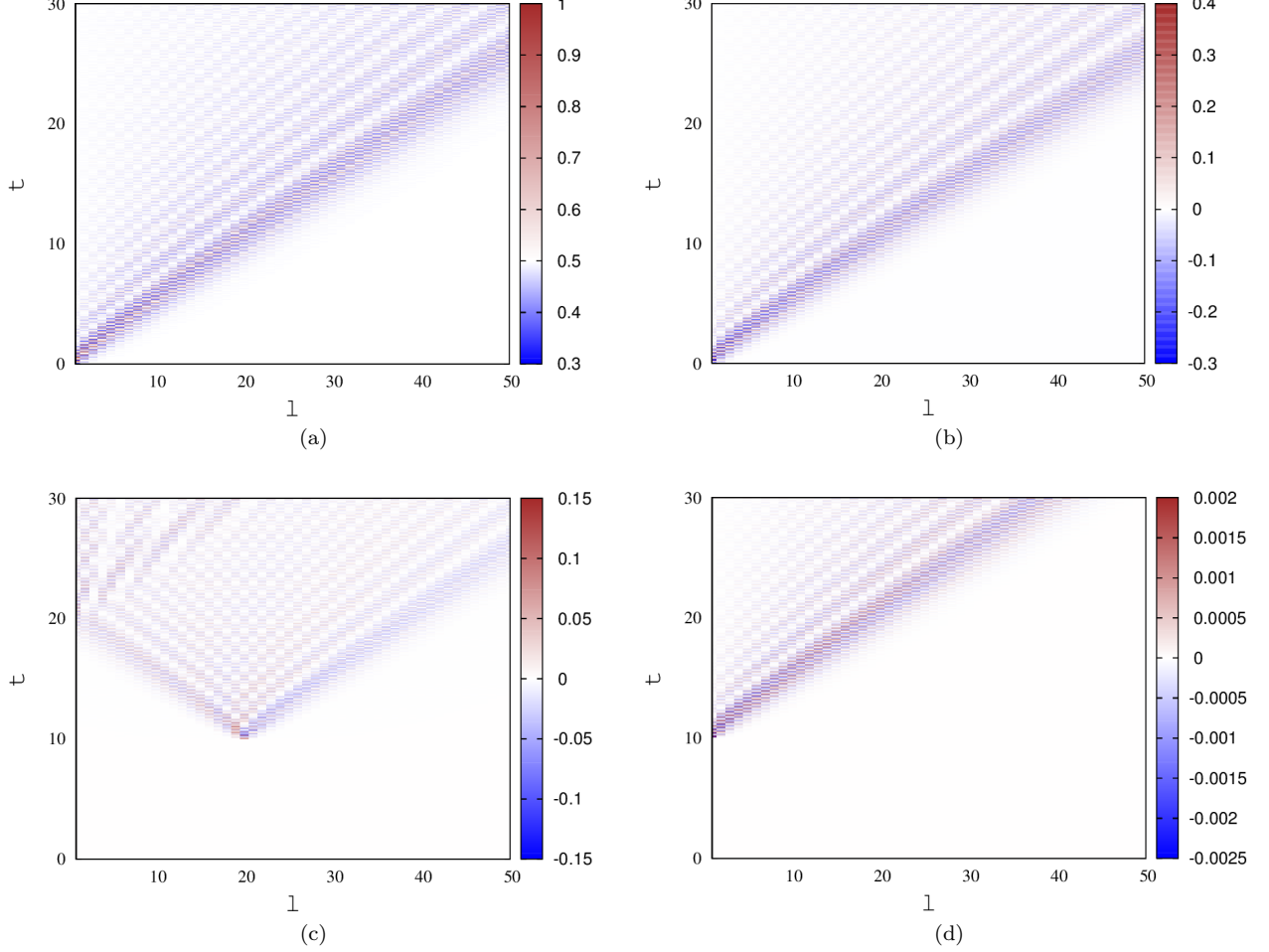


Figure 2. (a) State transfer fidelity $\mathcal{F}_l(t)$ as function of site index(l) and time (t) for Heisenberg dynamics with with open boundary condition without any decohering process. (b) Differences of state transfer fidelities with and without QDP ($\Delta\mathcal{F}_l, m = 1(t; t_0 = 0.0)$) as function of site index(l) and time (t); where the QDP occurs at the site ($m = 1$) and time ($t_0 = 0.0$). (c) $\Delta\mathcal{F}_l, m = 20(t; t_0 = 10.0)$ as function of site index(l) and time (t); where the QDP occurs at the site ($m = 20$) and time ($t_0 = 10.0$). $\Delta\mathcal{F}_l, m = 1(t; t_0 = 20.0)$ as function of site index(l) and time (t); where the QDP occurs at the site ($m = 1$) and time ($t_0 = 20.0$). Number of sites taken $N = 100$.

if the QDP is a coherent operation that will be discussed in the next section.

The initial state $\rho(0) = |\psi(0)\rangle\langle\psi(0)|$ undergoes three different evolutions here in three steps, as depicted in Fig.1 In the first step, the state is evolved through the unitary operation using the Heisenberg Hamiltonian. The evolution of the state up to $t = t_0^-$ results in the state, $\rho(t_0^-) = U_{t_0,0}\rho(0)U_{t_0,0}^\dagger$, where the unitary operator is given by $U_{t_2,t_1} = \exp -iH(t_2 - t_1)$, where we have absorbed the Planck constant in the time itself or set $\hbar = 1$. The state is given by,

$$\rho(t_0^-) = e^{-iHt_0}|\psi(0)\rangle\langle\psi(0)|e^{iHt_0} = |\psi(t_0)\rangle\langle\psi(t_0)|. \quad (18)$$

We have discussed the computation of $|\psi(t)\rangle$ in the last section, along with the state transfer fidelity. In the second step, an instantaneous operation of the local QDP

at the l 'th site, the state transforms from $\rho(t_0^-)$ to $\tilde{\rho}(t_0^+)$. Using the Kraus operator picture with the two operators P_0 and P_1 , the state is now given by

$$\tilde{\rho}(t_0^+) = P_0\rho(t_0^-)P_0^\dagger + P_1\rho(t_0^-)P_1^\dagger. \quad (19)$$

As we can see from the above, the state here is a mixed state with two different pure-state components, suffering decoherence due to the occurrence of the QDP at m 'th site. Just after the QDP, the state can be written in terms of two pure states as,

$$\tilde{\rho}(t_{0+}) = |\tilde{\psi}_+(t_0)\rangle\langle\tilde{\psi}_+(t_0)| + |\tilde{\psi}_-(t_0)\rangle\langle\tilde{\psi}_-(t_0)|, \quad (20)$$

where, $|\tilde{\psi}_\pm(t_0)\rangle \equiv \frac{1 \pm \sigma_m^z}{2}|\psi(t_0)\rangle$. In the third step, the state undergoes a unitary time evolution from $t = t_0^+$ to time t using the Heisenberg Hamiltonian, we have

$$\tilde{\rho}(t) = U_{t,t_0}\tilde{\rho}(t_0^+)U_{t,t_0}^\dagger. \quad (21)$$

In this step, the unitary Hamiltonian evolution occurs for an interval $t - t_0$. Finally, we can rewrite the state using the two pure states $|\tilde{\psi}^\pm\rangle$, as

$$\tilde{\rho}(t) = |\tilde{\psi}_+(t)\rangle\langle\tilde{\psi}_+(t)| + |\tilde{\psi}_-(t)\rangle\langle\tilde{\psi}_-(t)|, \quad (22)$$

where,

$$\begin{aligned} |\tilde{\psi}_+(t)\rangle &= \alpha e^{-i\epsilon_0 t} |00\dots 0\rangle + \beta \sum_{y'} H_1^{y'}(m, t, t_0) |y'\rangle, \\ |\tilde{\psi}_-(t)\rangle &= \beta \sum_{y'} K_1^{y'}(m, t, t_0) |y'\rangle, \end{aligned} \quad (23)$$

Here, the time-dependent wave functions[19] are given by,

$$\begin{aligned} H_y^{y'}(m, t, t_0) &= \sum_{y'' \neq m} G_y^{y''}(t_0) G_{y''}^{y'}(t - t_0), \\ K_y^{y'}(m, t, t_0) &= G_y^m(t_0) G_m^{y'}(t - t_0). \end{aligned} \quad (24)$$

Now, the elements of the time dependent RDM (given in Eq. 14) of the l^{th} site are given by,

$$\begin{aligned} \tilde{x}_l(t) &= \langle 1 | \tilde{\rho}_l(t) | 1 \rangle = |\beta|^2 (|H_1^l(m, t, t_0)|^2 + |K_1^l(m, t, t_0)|^2), \\ \tilde{y}_l(t) &= \langle 0 | \tilde{\rho}_l(t) | 1 \rangle = \alpha \beta^* e^{-i\epsilon_0 t} H_1^{*l}(m, t, t_0). \end{aligned} \quad (25)$$

The average state transfer fidelity averaged over all pure states on the Bloch sphere for l^{th} site is given by,

$$\begin{aligned} \tilde{\mathcal{F}}_{l,m}(t; t_0) &= \frac{1}{2} + \frac{1}{6} (|H_1^l(m, t, t_0)|^2 + |K_1^l(m, t, t_0)|^2) \\ &\quad + \frac{1}{3} \text{Re}(e^{i\epsilon_0 t} H_1^l(m, t, t_0)). \end{aligned} \quad (26)$$

The maximum fidelity saturates to the value $1/2$ over a long range because the function $G_1^l(t)$ is basically a Bessel function which falls as $1/t$. In case of a local decohering process the dynamics is not very different or in other words the QDP does not "disturb" the system significantly. Hence, the difference in fidelity with and without QDP for l^{th} site is given by $\Delta\mathcal{F}_{l,m}(t; t_0) = \tilde{\mathcal{F}}_{l,m}(t; t_0) - \mathcal{F}_l(t)$, we have

$$\begin{aligned} \Delta\mathcal{F}_{l,m}(t; t_0) &= \frac{1}{6} [|H_1^l(m, t, t_0)|^2 + |K_1^l(m, t, t_0)|^2 \\ &\quad - |G_1^l(t)|^2] + \frac{1}{3} \text{Re}(e^{i\epsilon_0 t} [H_1^l(m, t, t_0) - G_1^l(t)]). \end{aligned} \quad (27)$$

However, the quantum state transfer process (which is a coherent or unitary process) and the effect of the QDP (which is a decohering process) can interfere with each other and change the fidelity slightly. If the QDP is performed at a particular site at a time when the target state is at site while moving the fidelity changes slightly. From Eq. 27 the difference of fidelity with and without QDP can be estimated to be $\frac{1}{3} \text{Re}(e^{i\epsilon_0 t} G_1^l(t))$ at time

$t = l/2$.

The Fig. 2(b) depicts the change in fidelity for one extreme case where the QDP occurs at the first site just after the evolution starts. In that case the maximum difference in fidelity is around 0.4. However, when the QDP occurs at some other site at a later time this difference is much less. For example in Fig. 2(c) maximum change in fidelity is around 0.15 when the QDP is occurred at the site $m = 20$ at the time $t_0 = 10$. If the QDP occurs at a site where where the basic fidelity without the QDP itself is very small the inference effect is negligible and the fidelity does not change significantly. In Fig.2(d) depicts the case where the QDP occurs at the first site but at much later time $t_0 = 20.0$, the difference is seen to be negligible.

IV. LOCAL QUANTUM COHERENT PROCESS

In this section, we will turn our attention to the case of an instantaneous local unitary QDP intervening the unitary dynamics of the Heisenberg Hamiltonian. Similar to the last section, the QDP operates on the m 'th spin at time $t = t_0$. But unlike the previous section, the unitary QDP does not cause decoherence. The three steps of evolution that are involved here, as shown in Fig.1, are all unitary evolutions, as a result the initial pure state evolves into another pure state. The intervening QDP being unitary, it can be generated using a Hamiltonian. The instantaneous local unitary QDP intervening the unitary Hamiltonian evolution can be viewed as an evolution with a kicked Heisenberg Hamiltonian. The new Hamiltonian \tilde{H} can be written as a sum of two terms, the Heisenberg Hamiltonian H , given in Eq. 2 that generates the background unitary evolution, and a magnetic field term $H' = \vec{\sigma}_m \cdot \hat{n}$ with a delta-function kick, where \hat{n} is the direction of the magnetic field at the m 'th site. We can consider \hat{n} to be a unit vector in the x-y plane. Thus, the total Hamiltonian covering all the three steps can be written as,

$$\tilde{H} = H + H' \delta(t/t_0 - 1). \quad (28)$$

The second term in the Hamiltonian represents the instantaneous QDP operating on the given spin at $t = t_0$. The unitary evolution operator for $t > t_0$, is a product of three unitary operators corresponding to the three time steps, i.e., $U_{t_0,0} = e^{-iHt_0}$ for the evolution up to $t = t_0^-$, followed by $V_m = e^{-t_0 \vec{\sigma}_m \cdot \hat{n}}$ for the instantaneous unitary QDP, and $U_{t,t_0} = e^{-i(t-t_0)H}$ for the evolution from $t = t_0^+$ up to time t . Thus, an initial state $|\psi(0)\rangle$ prepared at time $t = 0$ evolves to the state $|\tilde{\psi}(t)\rangle = \tilde{U}_{t,0} |\psi(0)\rangle$, the evolution operator is given by,

$$\tilde{U}_{t,0} = U_{t,t_0} V_m U_{t_0,0}.$$

Now, similar to the non-unitary QDP, we start with an initial state $|\psi(0)\rangle = \alpha|0.0\rangle + \beta|100.0\rangle$. In the first

step, the state evolves unitarily upto a time t_0^- with the Hamiltonian H , yielding $|\psi(t_0^-)\rangle$. This part is the same as discussed in the last section, as shown in Eq. 10. In the second step, the state is changed by an operation of V_m , the m^{th} qubit undergoes a local unitary operation. This coherent or unitary process, which is a local quantum gate operation, is represented by an instantaneous unitary operation that acts on the state of the given qubit between time $t = t_0^-$ and time t_0^+ . The operation of the unitary operator V_m on the basis states of m^{th} spin is given by ,

$$V_m|0\rangle = \gamma|0\rangle + \delta|1\rangle, \quad V_m|1\rangle = -\delta^*|0\rangle + \gamma|1\rangle, \quad (29)$$

where the various amplitudes are related to t_0 , the components n_x, n_y of the unit vector \hat{n} as, $\gamma = \cos t_0$ and $(n_y + in_x) \sin t_0 = \delta$. The state $|\tilde{\psi}(t_0^+)\rangle$, immediately after the operation at $t = t_0$ is given by,

$$\begin{aligned} |\tilde{\psi}(t_{0+})\rangle &= V_m[\alpha e^{-i\epsilon_0 t_0}|F\rangle + \beta \sum_y G_1^y(t_0)|y\rangle] \\ &= (\alpha\gamma e^{-i\epsilon_0 t_0} - \beta\delta^* G_1^m(t_0))|F\rangle + (\alpha\delta e^{-i\epsilon_0 t_0} + \beta\gamma G_1^m(t_0))|m\rangle \\ &\quad + \beta\gamma \sum_{y' \neq m} G_1^{y'}(t_0)|y'\rangle + \beta\delta \sum_{y' \neq m} G_1^{y'}(t_0)|m, y'\rangle. \end{aligned} \quad (30)$$

Here, after the coherent operation, we can see that two-magnon states are also generating from one magnon states, that were absent in the last section. Now, the state is a mixture of zero, one and two magnon states. This is the simplest possible operation where three different magnon sectors are obtained. Each of these sectors will have their own dynamics, during the further evolution using the Heisenberg Hamiltonian, in the third step. The state at a later time t becomes,

$$\begin{aligned} |\tilde{\psi}(t)\rangle &= U_{t,t_0}|\tilde{\psi}(t_{0+})\rangle \\ &= (\alpha\gamma e^{-i\epsilon_0 t} - \beta\delta^* G_1^m(t_0)e^{-i\epsilon_0(t-t_0)})|F\rangle \\ &\quad + \sum_y [\alpha\delta e^{-i\epsilon_0 t_0} G_m^y(t-t_0) + \beta\gamma X_1^y(m, t, t_0)]|y\rangle \\ &\quad + \beta\delta \sum_{y_1, y_2; y_1 < y_2} L_{1,m}^{y_1, y_2}(m, t, t_0)|y_1, y_2\rangle. \end{aligned} \quad (31)$$

where we have used $X_1^n(m, t, t_0) = K_1^n(m, t, t_0) + H_1^n(m, t, t_0)$ to simplify the expression. where, the new time-dependent two-magnon sector wave function is given by,

$$\begin{aligned} L_{y',m}^{y_1, y_2}(m, t, t_0) &= \sum_{y'' > m} G_{y'}^{y''}(t_0) G_{m, y''}^{y_1, y_2}(t-t_0) \\ &\quad + \sum_{y'' < m} G_{y'}^{y''}(t_0) G_{y'', m}^{y_1, y_2}(t-t_0), \end{aligned} \quad (32)$$

in terms of the two-particle Green's function. The new Green's function is defined in terms of the two-magnon eigenfunctions $\psi_{p_1, p_2}(x_1, x_2)$, shown in Eq.5, and the

eigenvalues $\epsilon_2(p_1, p_2)$, we have,

$$G_{x_1, x_2}^{x'_1, x'_2}(t) = \sum_{p_1, p_2} \psi_{p_1, p_2}^{x_1, x_2} \psi_{p_1, p_2}^{x'_1, x'_2*} e^{-it\epsilon_2(p_1, p_2)}. \quad (33)$$

We have given the details of calculation of this Green's function both for two-magnon bound and scattering states in Appendix A.

Now, the matrix elements of the RDM of the l^{th} site, as given in Equation(12) , are modified with $\tilde{x}_l(t) = \frac{1}{2}\langle\tilde{\Phi}(t)|\mathbf{1} - \sigma_l^z|\tilde{\Phi}(t)\rangle$ and $\tilde{y}_l(t) = \langle\tilde{\Phi}(t)|\sigma_l^+|\tilde{\Phi}(t)\rangle$ of the RDM can be calculated from Equation(28) and are given by,

$$\begin{aligned} \tilde{x}_l(t) &= |\alpha\delta e^{-i\epsilon_0 t_0} G_m^l(t-t_0) + \beta\gamma X_1^l(m, t, t_0)|^2 \\ &\quad + |\beta|^2 |\delta|^2 \sum_{y' \neq l} |L_{1,m}^{l, y'}(m, t, t_0)|^2, \end{aligned} \quad (34)$$

and the off-diagonal matrix element is given by

$$\begin{aligned} \tilde{y}_l(t) &= e^{-i\epsilon_0(t-t_0)} (\alpha\gamma - \beta\delta^* G_1^m(t_0)e^{i\epsilon_0 t_0}) [\alpha^* \delta^* G_m^{*l}(t-t_0) + \\ &\quad \beta^* \gamma^* e^{-i\epsilon_0 t_0} X_1^{*l}(m, t, t_0)] + \sum_{y \neq l} (\alpha\beta^* |\delta|^2 e^{-i\epsilon_0 t_0} G_m^y(t-t_0) \\ &\quad + |\beta|^2 \gamma \delta^* X_1^y(m, t, t_0)) L_{1,m}^{*l, y}(m, t, t_0). \end{aligned} \quad (35)$$

After averaging over all pure states on the Bloch sphere average state transfer fidelity for l^{th} site is given by,

$$\begin{aligned} \tilde{\mathcal{F}}_{l,m}(t; t_0) &= \frac{1}{2} + \frac{|\gamma|^2}{6} [|X_1^l(m, t, t_0)|^2 \\ &\quad + 2\text{Re}(e^{-i\epsilon_0 t} X_1^{*l}(m, t, t_0))] + \frac{|\delta|^2}{6} [\sum_{y \neq l} |L_{1,m}^{l, y}(m, t, t_0)|^2 \\ &\quad - |G_m^l(t-t_0)|^2 + 2\text{Re}(\sum_{y \neq l} e^{-i\epsilon_0 t_0} G_m^y(t-t_0) L_{1,m}^{*l, y}(m, t, t_0))]. \end{aligned} \quad (36)$$

The special case where $\gamma = \alpha$ and $\delta = \beta$ average state transfer fidelity for l^{th} site is expected to be maximum and given by,

$$\begin{aligned} \tilde{\mathcal{F}}_{l,m}^{\text{max}}(t; t_0) &= \frac{1}{2} + \frac{1}{6} \left\{ \sum_{y \neq l} |L_{1,m}^{l, y}(m, t, t_0)|^2 + \text{Re} e^{-i\epsilon_0 t} X_1^{*l} \right. \\ &\quad \left. + \text{Re} \sum_{y \neq l} [e^{-i\epsilon_0 t_0} G_m^y(t-t_0) + X_1^y] L_{1,m}^{*l, y}(m, t, t_0) \right\}, \end{aligned} \quad (37)$$

Unlike the previous case here quantum state transfer will be contributed by both the magnon bound states and scattering states sectors. We can try to analyse how much contribution to the fidelity comes from two magnon scattering states and two magnon bound states. Hence, the time dependent function $G_{x_1, x_2}^{x'_1, x'_2}(t)$ can be split into two parts $G_{(B); x_1, x_2}^{x'_1, x'_2}(t)$ and $G_{(S); x_1, x_2}^{x'_1, x'_2}(t)$ corresponding to contributions from bound states and scattering states respectively. It is known that for a

chain with N sites number of two magnon bound states is of the order of N where as, number of two magnon scattering states is $O(N^2)$.

The dependence of the state transfer fidelity on the target site location and time has been shown as density plots in Fig.3 for the Heisenberg dynamics with a unitary QDP. Fig. 3(a) and Fig. 3(b) show the contribution to the state transfer fidelity from the two-magnon bound states and the scattering states respectively. We can see that the contribution of the two-magnon scattering states is larger than the contribution coming from the two-magnon bound states. This is according to our expectation, as the number of bound states is N , whereas there are $O(N^2)$ number of scattering states. The difference in the fidelities $\Delta\mathcal{F}$ of the two states, $\tilde{\rho}(t)$ and $\rho(t)$, is shown as a density plot in Fig.3(c) as a function of l and t . It can be seen from here that it can take both positive and negative values, corresponding to constructive and destructive interference of the propagation of the coded information at $t = 0$ and the unitary QDP occurring at $t = t_0$. The more interesting regime is where the fidelity difference is positive and is around 0.2, implying a 20 per cent increase in the probability of the state transfer, coming from the implementation of the QDP at a single site. It is important to state here that this increase occurs only for the case, the coded state arrives at the location of QDP, viz. site m at the time $t = t_0$, to take the maximum benefit of the interference. We have shown the difference in the fidelities in Fig. 3(d) as a function of the target site l , for various values of the interaction parameter Δ of the Hamiltonian. We can see it is fluctuating around 0.1 for all parameter values, implying a similar behaviour. The amplitude of the fluctuations is maximum for the case of $\Delta = 0$, corresponding to the XY model.

An interesting case can be studied when the first qubit undergoes the local operation just after the evolution starts. As a consequence it can be seen from Equation(30) that the contribution from two magnon sector becomes zero because of the term $G_1^y(0)$. The Eq. 36 and Eq.37 then reduce to respectively,

$$\begin{aligned}\tilde{\mathcal{F}}_{l,m=1}(t; t_0 = 0_+) &= \frac{1}{2} + \frac{1}{6}(|\gamma|^2 - |\delta|^2)|G_1^l(t)|^2 \\ &+ \frac{|\gamma|^2}{3}Re((e^{i\epsilon_0 t}G_1^l(t)), \\ \tilde{\mathcal{F}}_{l,m=1}(t; t_0 = 0_+) &= \frac{1}{2} + \frac{1}{6}Re((e^{i\epsilon_0 t}G_1^l(t)).\end{aligned}\quad (38)$$

The last terms of the above equations are merely oscillating terms. Second Equation suggests that state transfer will not take place. Setting $|\gamma| = |\delta|$ (Hadamard gate operation)in the first one also shows the same.

The speed of state transfer is if the order of J (here J is taken to be $1/2$). Another interesting case can be studied where $t_0 = Jt = l/2$, which means that the evolution is interrupted at a particular site when the target state is

passing through. In context of quantum state transfer where the target state is unknown at the receiver end one can vary the parameters γ and δ to get the maximum fidelity. The values of m , t_0 and t is set l , $l/2$ and $l/2$ respectively in Eq.36. Maximum value of the fidelity can be obtained when $\gamma = 0$ and $\delta = 1$ (bit flip or X gate)for large values of l and the difference in fidelity with and without the local operation is given by,

$$\begin{aligned}\Delta\mathcal{F}_{l,m=l}(t = \frac{l}{2}; t_0 = \frac{l}{2}) &= \tilde{\mathcal{F}}_{l,m=l}(t = \frac{l}{2}; t_0 = \frac{l}{2}) - \mathcal{F}_l(t = \frac{l}{2}) \\ &= \frac{1}{6}[\sum_{y \neq l} |L_{1,l}^{l,y}(m = l, t = \frac{l}{2}, t_0 = \frac{l}{2})|^2 - |G_m^l(t = \frac{l}{2})|^2 \\ &- 2Re(e^{i\epsilon_0 l/2}G_1^l(t = \frac{l}{2})) - 1].\end{aligned}\quad (39)$$

Whereas, from Eq.37 the maximum fidelity occurs for $m = l$ and $t = t_0 = l/2$, is given by,

$$\begin{aligned}\mathcal{F}_{l,m=l}^{max}(\frac{l}{2}, \frac{l}{2}) &= \frac{1}{2} + \frac{1}{6}\{\sum_{y \neq l} |L_{1,l}^{l,y}(l, \frac{l}{2}, \frac{l}{2})|^2 + \frac{1}{6}Re[e^{i\epsilon_0 l/2}K_1^{*l}(l, \frac{l}{2}, \frac{l}{2}) \\ &+ \sum_{y \neq l} H_1^l(l, \frac{l}{2}, \frac{l}{2})L_{1,l}^{*l,y}(l, \frac{l}{2}, \frac{l}{2})]\}.\end{aligned}\quad (40)$$

V. LOSCHMIDT ECHO

An isolated system evolves unitarily which allows a pure state to remain pure. So, such systems can be brought back to their initial state through time reversal operation. If the system interacts with the environment this is no longer true and Such systems cannot be brought back to their initial state by time reversal unitary operation. However, it has been proposed that the probability of restoring the system to the initial state is a decreasing function of time. Peres [20] first showed that classically chaotic and integrable system behave differently under imperfect time reversal.

The Loschmidt Echo is a measure of the revival of the state when an imperfect time reversal procedure is applied during the evolution of a quantum system. It quantifies the sensitivity of the quantum state to the local decohering process. The Loschmidt Echo has been studied in many body systems and it has been observed that it decays exponentially in ergodic systems. The time scale can be related to the Lyapunov exponent of the classical system [26, 30, 31].

In our case after the local instantaneous local operation on the system will not be able to revive to the initial state if the time reversal unitary process is performed. Here, in next sections we will study the dynamics of many qubit systems (both integrable and

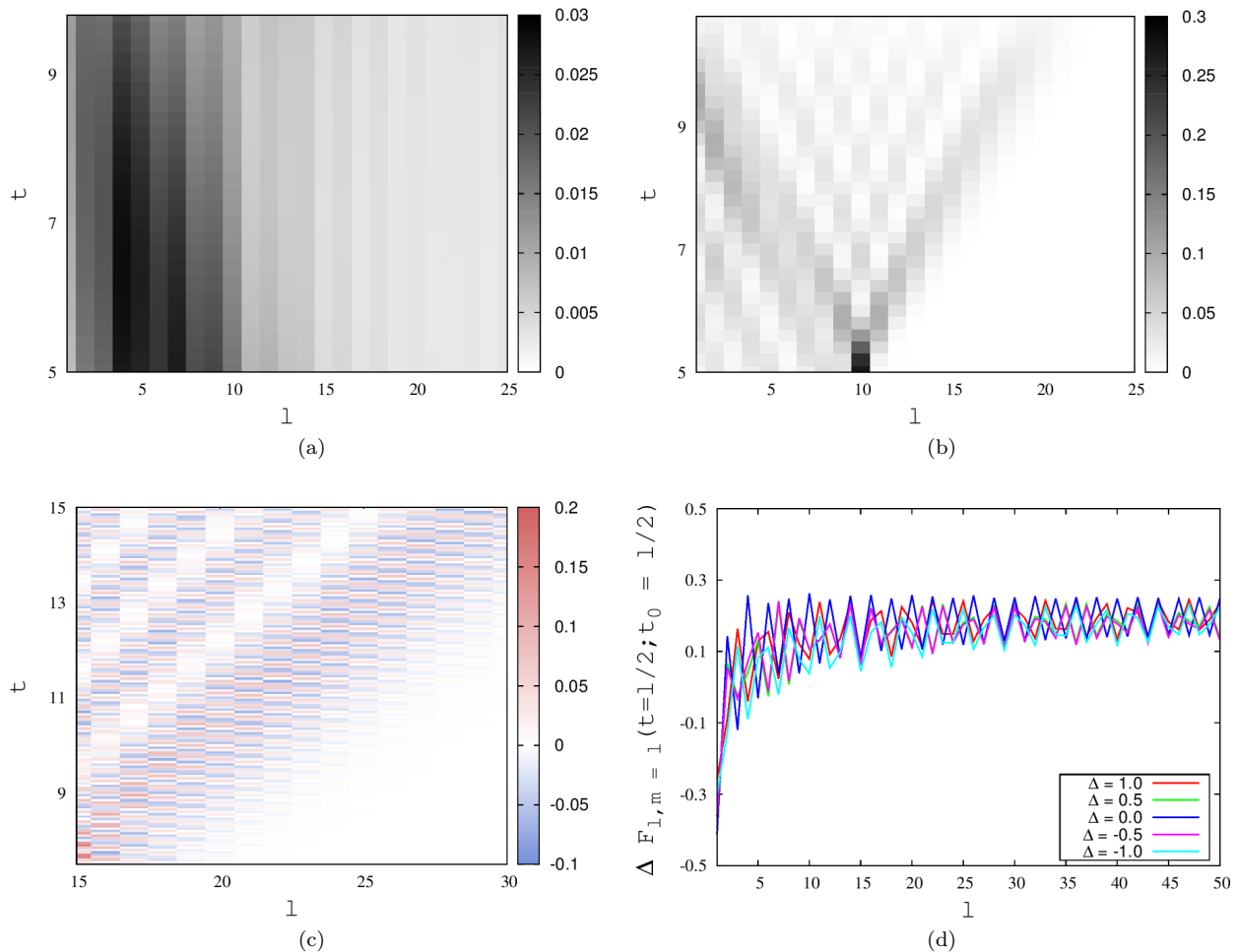


Figure 3. (a) $\frac{1}{6} \sum_{y' \neq l} |L_{1,m}^{l,y'}(m, t, t_0)|^2$ as function of site index(l) and time (t) for Heisenberg dynamics with closed boundary condition with local unitary operation on the tenth site at $t_0 = 5.0$. without taking two magnon scattering states into account for anisotropy constant $\Delta = 1.0$.(b) $\frac{1}{6} \sum_{y' \neq l} |L_{1,m}^{l,y'}(m, t, t_0)|^2$ as function of site index(l) and time (t) for Heisenberg dynamics with closed boundary condition with local unitary operation on the tenth site at $t_0 = 5.0$. without taking two magnon bound states into account for anisotropy constant $\Delta = 1.0$.(c) $\Delta \mathcal{F}_{l,m=15}(t; t_0 = 7.5)$ as function of site index(l) and time (t) for Heisenberg dynamics with closed boundary condition with local unitary operation on the tenth site at $t_0 = 7.5$ for anisotropy constant $\Delta = 1.0$. (d) $\Delta \mathcal{F}_{l,m=1}(t=l/2; t_0=l/2)$ as function of site index l for different values of anisotropy constants Δ .

non-integrable) under local instantaneous operations in the context of quantum state transfer. In our context the Loschmidt Echo is defined as the probability of the state to return to its initial state by time reversal unitary process after the operation which occurs at t_0 . It is quantified by taking overlap of the time reversal state with the initial state as a function of time. In our case, the state evolves unitarily after the incoherent QDP the Loschmidt Echo will not be a function of time but a function of the time of occurrence of the QDP and in general the site index m where it occurs.

The Loschmidt echo, for unitarily evolved states, is just the overlap of the two states evolved under two different Hamiltonians. The two evolutions we discuss here, with and without the QDP, give two final states $\tilde{\rho}(t)$

and $\rho(t) = |\psi(t)\rangle\langle\psi(t)|$ respectively. The state with a non-unitary QDP, discussed in Section III, is a mixed state. For accommodating this aspect, we can generalise the definition of the Loschmidt Echo $S(m, t_0)$ as,

$$S(m, t_0) = \text{Tr} \tilde{\rho}(t) \rho(t) = \langle \psi(t) | \tilde{\rho}(t) | \psi(t) \rangle. \quad (41)$$

Though, the overlap of the two states is taken at time t , the Loschmidt echo will depend only on t_0 , as the two evolutions are same except at $t = t_0$. Now, depending on the QDP being a non-unitary or unitary, we can calculate $S(m, t_0)$ using the dynamics of the initial state that we discussed in the last two chapters. For the non-unitary QDP, the state $\tilde{\rho}(t)$ is calculated from Eq. 19 and 21. The state pure state $\rho(t)$ is given by the state $|\psi(t)\rangle = U_{t,0}|\psi(0)\rangle$. Using these, we can simplify the ex-

pression for the Loschmidt echo, displaying explicitly the dependence on m and t_0 , using the projection operators shown in Eq. 19, we have

$$\begin{aligned} S(m, t_0) &= |\langle \psi(t_0) | P_0 | \psi(t_0) \rangle|^2 + |\langle \psi(t_0) | P_1 | \psi(t_0) \rangle|^2 \\ &= \frac{1}{2} + \frac{1}{2} |\langle \psi(t_0) | \sigma_m^z | \psi(t_0) \rangle|^2 = \frac{1}{2} + \frac{1}{2} |\langle \psi(0) | U_{0,t_0} \sigma_m^z | \psi(t_0) \rangle|^2. \end{aligned} \quad (42)$$

It shows that the probability can not be less than half for the model of incoherent QDP chosen. We will take Heisenberg Dynamics as a representative of an integrable dynamics and see how the quantity $S_m(t_0)$ depends on t_0 and the site where it occurs. From equation(10) we can write,

$$U_{0,t_0} \sigma_m^z | \psi(t_0) \rangle = \alpha | F \rangle + \beta \sum_y (M_1^y(m, t_0) - N_1^y(m, t_0)) | y \rangle. \quad (43)$$

Here, the new time-dependent wavefunctions are given by,

$$\begin{aligned} M_y^{y''}(m, t_0) &= \sum_{y' \neq m} G_y^{y'}(t_0) G_{y''}^{*y'}(t_0), \\ N_y^{y''}(m, t_0) &= G_y^m(t_0) G_{y''}^{*m}(t_0). \end{aligned} \quad (44)$$

Hence, the expression for $S_m(t_0)$ calculated from Equation(42) is given by,

$$S(m; t_0) = \frac{1}{2} + \frac{1}{2} (|\alpha|^2 + |\beta|^2 Z_1^1(m, t_0))^2, \quad (45)$$

where we have defined $Z_1^1(m, t_0) = M_1^1(m, t_0) - N_1^1(m, t_0)$ for simplifying the above expression. The average Loschmidt Echo averaged over all pure states on the Bloch sphere is given by,

$$S(m; t_0) = \frac{2}{3} + \frac{1}{6} |Z_1^1(m, t_0)|^2 + \frac{1}{6} \text{Re} Z_1^1(m, t_0). \quad (46)$$

The Loschmidt Echo can be straightforwardly written for the coherent QDP discussed in Section IV, in terms of the state at t_0 and the instantaneous local gate operators, as

$$\begin{aligned} S(m; t_0) &= |\langle \psi(t) | \tilde{\psi}(t) \rangle|^2 = |\langle \psi(t_0) | \tilde{\psi}(t_0^+) \rangle|^2 \\ &= |\langle \psi(0) | U_{0,t_0} | \tilde{\psi}(t_0^+) \rangle|^2 = |\langle \psi(t_0) | V_m | \psi(t_0) \rangle|^2. \end{aligned} \quad (47)$$

In the last step, we have written it as the overlap of $|\tilde{\psi}(t_0^+)\rangle$, and the state obtained from the time-reversed unitary process from t_{0+} to 0. The dependence of $S(m, t_0)$ on the m and t_0 is more transparent, in the above, when it is written as the squared expectation value of V_m in the state $|\psi(t_0)\rangle$. The time-reversed state can be calculated as,

$$\begin{aligned} U_{0,t_0} |\tilde{\psi}(t_{0+})\rangle &= (\alpha\gamma - \beta\delta^* e^{i\epsilon_0 t_0} G_1^m(t_0)) | F \rangle \\ &+ \alpha\delta e^{-i\epsilon_0 t_0} \sum_{y'} G_{y'}^{*m}(t_0) | y' \rangle + \beta\gamma \sum_{y'} (M_1^{y'}(m, t_0) \\ &+ N_1^{y'}(m, t_0)) | y' \rangle + \sum_{y_1, y_2: y_1 < y_2} P_1^{y_1, y_2}(m, t_0) | y_1, y_2 \rangle. \end{aligned} \quad (48)$$

Even after the time reversal the state contains zero, one and two magnon sectors. Since the initial state is a combination of zero and one magnon states the two magnon sector does not contribute to the Loschmidt echo. Hence the probability to revive the initial state is always less than one. The expression for the Loschmidt echo as a function of t_0 is given as,

$$\begin{aligned} S(m; t_0) &= \left| |\alpha|^2 \gamma + |\beta|^2 \gamma (M_1^1(m, t_0) + N_1^1(m, t_0)) \right. \\ &\left. + \alpha\beta^* \delta e^{-i\epsilon_0 t_0} G_1^{*m}(t_0) - \alpha^* \beta \delta^* e^{i\epsilon_0 t_0} G_1^m(t_0) \right|^2. \end{aligned} \quad (49)$$

For large value of t_0 value of $S(m; t_0)$ saturates to $|\gamma|^2/3$. Hence, the value of the Loschmidt echo for large value of t_0 cannot exceed $1/3$. For different coherent operations this value is different. For X gate, Y gate the value is zero; for Hadamard gate it is $1/6$ and Z gate the value is $1/3$ which is maximum. However, for the special case where $\gamma = \alpha$ and $\delta = \beta$ the average Loschmidt Echo averaged over all pure states on the Bloch sphere is given by,

$$S(m; t_0) = \frac{1}{4} + \frac{1}{12} [Y_1^1(m, t_0) + 2\text{Re} Y_1^1(m, t_0)], \quad (50)$$

where we the new function is related to the various Green's functions by,

$$Y_1^1 = M_1^1(m, t_0) + N_1^1(m, t_0) + 2Im e^{-i\epsilon_0 t_0} G_1^{*m}(t_0). \quad (51)$$

The Fig. 4(a) depicts the variation of the Loschmidt echo as a function of t_0 for different values of m and chain size N for incoherent QDP. The Fig. 4(b) depicts the same for coherent QDP. In both these cases it can be seen that $S(m, t_0)$ remains almost constant and after a certain time it starts decaying with the value of t_0 . The maximum value of t_0 up to which it remains flat is exactly equal to the time taken by the state to reach the other end of the chain. In case of incoherent QDP (the decohering process) the value remains almost unity upto $t_0 = N/2$ with small fluctuations which can be seen from Fig. 4(a). This implies that the system can almost be revived to its initial state before the state reaches to the other end of the chain. But in case of coherent interrupting QDP the state obtained after the operation is a combination of zero, one and two magnon states and each sector has its own conserved dynamics. So, the probability of reviving the system to the initial state is always less than one which can be seen from figures 4(b) and

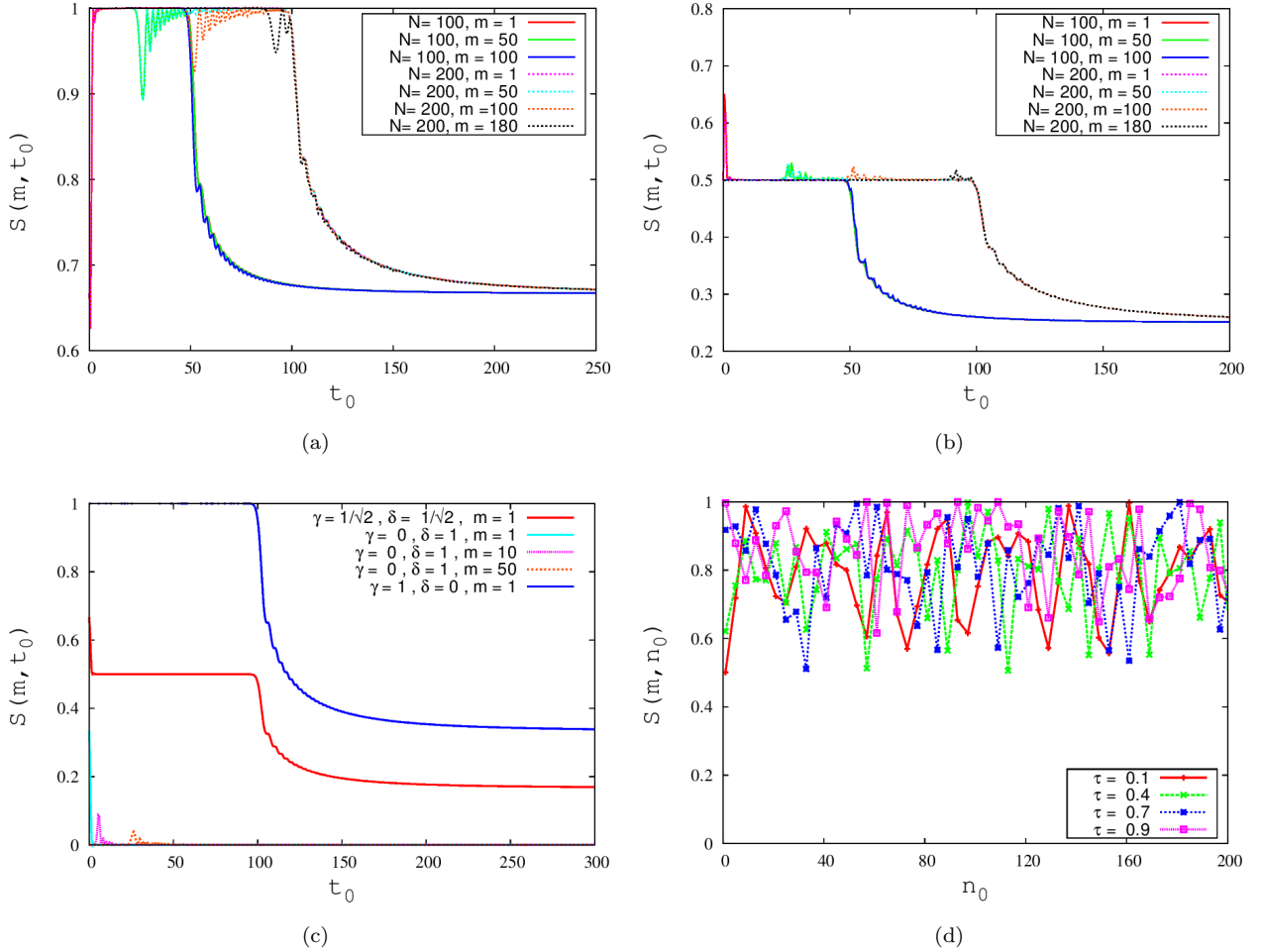


Figure 4. The Loschmidt Echo $S(m, t_0)$ is plotted for Heisenberg dynamics with open boundary condition for different m values as function of local incoherent QDP time t_0 (a) for incoherent process and (b) unitary local gate operation, (c) For different values of γ and δ for $N = 200$. (d) The Loschmidt Echo $S(m, n_0)$ is plotted for kicked Harper dynamics with open boundary condition for different values of τ with $m = 1$ for system size $N = 10$. n_0 is the number of steps after the QDP occurs.

4(c). Beyond the value $t_0 = N/2$ the Loschmidt echo decays with time reaches asymptotically to the values $2/3$ for incoherent QDP and different values for unitary QDP operations depending on the values of γ and δ respectively. $S(m, t_0)$ is shown in Fig. 3(c) as a function of t_0 for different values of γ and δ and m are plotted for a fixed system size $N = 200$. This can be easily seen from Eqs. (46), (49) and (50), and Fig. 4(c). These numbers depends on the type of interruptions. Also in both the cases some fluctuations are observed around the time $t_0 = m/2$ when the interruption process is performed at the m^{th} site. Which may be the signature that the target state is passing through that site. The variation of Le as a function of n_0 (number of kicks before the QDP occurs) and m for four different values of τ . In contrast to Heisenberg dynamics no constant decay is seen in the value of the Loschmidt echo as a function of t_0 . Also the values show more fluctuations which may be the results

of a small size system.

VI. LOCAL DECOHERING PROCESS IN NON-INTEGRABLE QUANTUM SYSTEMS

In the previous sections, we have considered the effect of an intervening QDP, either non-unitary or unitary, on the background unitary Hamiltonian evolution, governed by the Heisenberg Hamiltonian, that belongs to the integrable class of dynamical systems. It will be interesting to see the effect of a QDP intervention on a unitary evolution, corresponding to non-integrable Hamiltonian systems. The signal propagation from a local QDP and its detection with a background non-integrable dynamics has been investigated in XY model with transverse and longitudinal magnetic fields[19]. The Loschmidt echo is also sensitive to the dynamics being integrable or non-

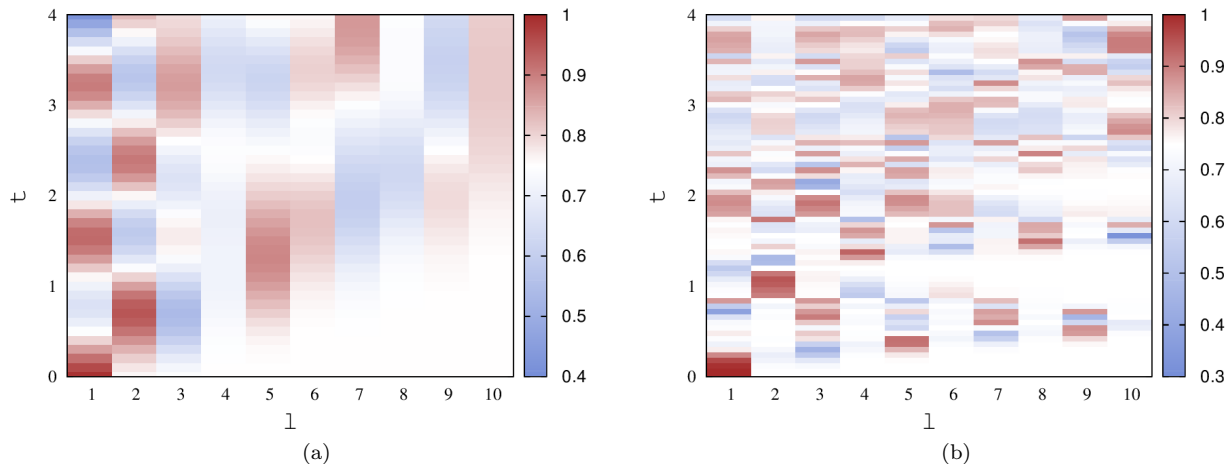


Figure 5. The state transfer fidelity $\mathcal{F}_l(t)$ as function of site index(l) and time (t) for kicked Harper dynamics with open boundary condition with parameters (a) $g = 1.0$ and $\tau = 0.1$, (b) $g = 1.0$ and $\tau = 0.9$, $\eta = \sqrt{2}$ for each case. The initial state in both the cases is $|\psi(0)\rangle = \sqrt{0.75}|00\dots 0\rangle + \sqrt{0.25}|100\dots 0\rangle$.

integrable[20]. Moreover, there are sharp differences in the eigenvalue spacing distribution and the structure of the eigenfunctions in the two cases, that have been widely investigated. To see the effect of QDP in non integrable systems we consider a simple model Hamiltonian with a tuneable parameter, to go continuously from completely integrable to completely non-integrable regimes. We use a one-dimensional periodically-kicked Harper model, a simple model of fermions hopping on a chain with an inhomogeneous site potential, appearing as a kick at regular intervals. The Hamiltonian is given by

$$H(t) = \sum_{j=1}^N \hat{c}_j^\dagger \hat{c}_{j+1} + g \cos\left(\frac{2\pi j \eta}{N}\right) \hat{c}_j^\dagger \hat{c}_j \sum_{n=-\infty}^{\infty} \delta(t/\tau - n), \quad (52)$$

where \hat{c}_j^\dagger is a creation operator at site j , g is a potential strength parameter, η is a parameter to make the potential either commensurate or incommensurate with the lattice, and τ is the kicking interval. The first term represents the kinetic energy of the fermion or hopping term, and the second term is the kicked potential energy operator. The Hilbert space for a site is two-dimensional, either occupied site or unoccupied site, thus it can be mapped to the spin language. The first term will turnout to be XY term, shown in In the Eq.2, and the second term becomes a transverse field that is inhomogeneous. The fermion occupation can be mapped to the down spin occupation in the spin states. Unlike the Heisenberg Hamiltonian that incorporates an interaction of down spins on neighbouring sites, there are no many-body interaction effects here. The kicked Harper model has been investigated for the entanglement distribution and dynamics[23]. The effect of the magnetic field or the potential is through a train of kicking pulses with an interval τ . For $\tau \rightarrow 0$ the dynamics of the Harper

Hamiltonian is integrable, and for large values of τ the dynamics is completely chaotic (see Figure 4 in the work of Lakshminarayan and Subrahmanyam[23] for further details)[24].

Similar to the previous sections, we will consider an initial state $|\psi_0\rangle = \alpha|00\dots 0\rangle + \beta|10\dots 0\rangle$, a linear combination of zero-particle state and one-particle state localised at first site. Through the time evolution, the particle can hop around to other sites. We will consider evolution at discrete times, viz. $t = \tau^+, 2\tau^+$ etc, that is at instant just after a kick. The evolution operator U_n at a time just after n kicks (corresponding to $t = n\tau$), is given by

$$U(n) = \left(e^{-i\tau \sum_j c_j^\dagger c_{j+1}} e^{-i\tau g \sum_j \cos\left(\frac{2\pi j \eta}{N}\right) c_j^\dagger c_j} \right)^n, \quad (53)$$

where the two operator factors appearing above do not commute. This evolution operator evolves the initial state to give $|\psi_n\rangle = U(n)|\psi_0\rangle$.

The above unitary evolution is intervened by a local instantaneous non-unitary QDP, as considered in Section III, at time $t = n_0\tau^+$. Thus, the evolution proceeds in three steps as shown in Fig. 1. In the first step, the initial state will become the state $|\psi(n_0)\rangle$ at time $t = n_0\tau$. In the second step, the state $\rho(n_0)$, in analogy with Eq. 17, will result in the state $\tilde{\rho}(n_0) = P_0\rho(n_0)P_0^\dagger + P_1\rho(n_0)P_1^\dagger$. The third step, the state evolves unitarily to become,

$$\tilde{\rho}(n) = U(n-n_0)(P_0\rho(n_0)P_0^\dagger + P_1\rho(n_0)P_1^\dagger)U^\dagger(n-n_0). \quad (54)$$

Unlike in the previous sections, we cannot proceed analytically, in the absence of exact solutions for the eigenstates of the Hamiltonian. We can calculate the action of the various unitary operators numerically for a finite chain of $N = 10$ sites. We have calculated numerically the Loschmidt echo $S(m, n_0)$, where m stands for the location of the local QDP occurrence, and n_0 is the time at

which it occurs. The Loschmidt echo for non-integrable case (for a few values of τ between 0.1 and 0.9), has been shown in Fig. 4(d) as a function of n_0 . The Loschmidt echo in this case is in sharp contrast with that of Heisenberg dynamics shown in Fig. 4(a)-4(c). The oscillatory structure may be a finite-size effect, but it oscillates at a higher value of 0.8, compared to the Heisenberg dynamics, where $S(m, t_0)$ levels off to a smaller value for large t_0 , as expected[20]. The quantum state transfer fidelity can also be calculated numerically, by calculating the matrix elements of the reduced density matrix $\rho_l(n)$ for the l 'th site, noting that \tilde{x}_l is just the expectation value of the fermion number operator. We have, analogous to Eq. 27,

$$\tilde{x}_l(n) = Tr c_l^\dagger c_l \tilde{\rho}(n), \quad \tilde{y}_l(n) = Tr c_l^\dagger \tilde{\rho}(n), \quad (55)$$

where we have written the matrix elements as expectation value of operators. The state transfer fidelity can be calculated numerically using the above. The average fidelity in this case has been shown in Fig. 5(a) for a smaller value of $\tau = 0.1$ and in Fig. 5(b) for $\tau = 0.9$ as a density plot, for various target sites and times. For a smaller τ , the dynamics is still closer to an integrable one. For small times, we can see larger fidelity only for small l . As the time increases, for larger values of l get larger fidelity (around 0.8). This is as expected, the state is spreading at a given speed. However, for larger value of τ shown in Fig. 5(b), even for small times too there are larger fidelities for far away sites. This implies, we cannot define a speed of propagation for the non-integrable case. Similar features were seen in XY model with transverse and longitudinal fields[19].

We will define and study a detector function given by,

$$f_l(t = n\tau) = \tilde{x}_l(t) - x_l(t). \quad (56)$$

Here, the two quantities are the diagonal matrix elements of the RDM from the two states $\tilde{\rho}(n)$ and $\rho(n)$ evolved with and without the QDP occurrence. This is a useful detector function to see the effect of the QDP, similar to the Loschmidt echo, but a lot simpler to calculate. This function has been studied in detail for various Hamiltonians in conjunction with a non-unitary QDP[19]. One can also study similar detector functions constructed from the off-diagonal matrix elements, and the von-Neumann entropy of the RDM. It has been seen that they all show similar structure. The results for the above detector function are shown in Fig. 6(a) to Fig. 6(f) for various combination of values for g and τ .

For smaller values of kicking interval τ and potential strength g the detector function $f_l(t)$ shows behaviour similar to that of integrable models like Heisenberg model, XY model with transverse magnetic field [19]. The signal of the local QDP propagates through the chain with a finite speed which is shown in Fig. 76a). But the qualitative nature of the detector function depends on both the parameters τ and g . If the value of g is increased the signal propagation does not take place

or in other words $f_l(t)$ is zero for farther sites. This is depicted in Fig. 6(b), Fig. 6(c) and Fig. 6(e). For larger values of τ the speed of propagation abruptly becomes very high, which can taken as a signature of transition from integrability to non integrability. Fig. 6(d) shows this for $\tau = 0.4$ and $g = 1$. For $\tau = 0.9$ the signal travels very quickly to the other end of the chain and, thus, it is difficult to define a finite speed in this case as it is shown in Fig. 6(f). Similar behaviour we have seen for the state transfer fidelity in Fig. 5. We can say that for $g > 1$ and smaller value of τ , the signal does not propagate to larger distances, and we cannot define a speed, as shown in Fig.6(b), (c) and (e). On the other hand, for $g = 1$, and larger values of τ , as seen in Fig. 6(d) and (f), the signal spreads out almost instantaneously to larger distances, and we cannot get a finite speed. We can connect this feature of the detector function with the oscillatory structure seen in the Loschmidt echo in Fig. 4(d).

VII. CONCLUSIONS

In this paper, we have investigated the effect of a local quantum dynamical process (QDP), both unitary and non-unitary processes, intervening the process of quantum state transfer through a unitary evolution for both integrating and non integrating models. For Heisenberg model, that represents an integrable dynamics, we have analytically calculated the state transfer fidelity in terms of time-dependent Green functions. The information coded in the state of the first spin, spreads out to other location through the unitary dynamics, We have seen that the signal from the local QDP can interfere with the dynamics of the state transfer, and it changes the fidelity depending on the time and the location of the QDP. In the case of a non-unitary QDP, there is a small change in the state transfer fidelity, even if the QDP occurs at the location of the particular qubit where the coded state arrives at the time of QDP. However, for a coherent or unitary QDP, the fidelity can increase or decrease depending on the constructive or destructive interference of the propagation of the coded state, and the signal from the QDP. For appropriate location and the time, the state transfer fidelity can increase substantially. In the case of unitary QDP, an initial state with a combination of zero and one-magnon states, becomes a superposition of zero, one and two magnon eigenfunctions. The state transfer has contributions from both two-magnon bound states and scattering states, which are quantitatively calculated separately using the two-magnon Bethe ansatz wave functions.

We have investigated the Loschmidt Echo, that quantifies the overlap of the time-reversed quantum state with the initial state, with no QDP during the time reversal, is quite capable of isolating the effect of the QDP, from the background dynamics. Also, it is sensitive to whether the background dynamics is integrable or non-

integrable. Here, we have seen that the Loschmidt echo is constant upto a certain time, and then decays and saturates to a certain value depending on that parameters in the QDP for integrable systems. We have considered a kicked Harper model as an example of a non-integrable dynamics. In this case, the Loschmidt echo shows oscillatory behaviour for non integrable systems, in a sharp contrast with the integrable dynamics.

Finally, we have investigated the dynamics of Kicked Harper model in the context of quantum state transfer. The dynamics of this model changes from integrable to non integrable by increasing the kicking interval time. We show that the spreading of the coded state is dependent on the kicking interval time. For smaller values of τ the dynamics is similar to the integrable model and larger values of τ the spreading takes place quickly which is a possible signature of non integrability. The signal propagation also depends on the potential strength parameter g and τ . The signal propagates with a finite speed below a certain value of τ and above that value the propagation takes place too quickly to define a speed. Whereas, for larger value of g the signal does not reach the farther sites. So, the signal of the QDP gets localised.

Acknowledgement: SS acknowledges the financial support from CSIR, India. We thank Professor A. Lakshminarayan for useful discussion of non-integrable systems.

Appendix A

The time-dependent two-particle Green's function $G_{x_1, x_2}^{x'_1, x'_2}(t)$ has contributions from both scattering and bound states. We can write the function as two parts, as

$$G_{x_1, x_2}^{x'_1, x'_2}(t) = G_{(B); x_1, x_2}^{x'_1, x'_2}(t) + G_{(S); x_1, x_2}^{x'_1, x'_2}(t). \quad (57)$$

In Bethe Ansatz solution for the two-magnon eigenfunctions for a chain with periodic boundary conditions, the momenta can be parametrised by the relation,

$$p_i = 2 \cot^{-1}(2\lambda_i). \quad (58)$$

The S-matrix in the Bethe Ansatz wave function is given in the form,

$$S(p_1, p_2) = e^{i\theta(p_1, p_2)}, \quad (59)$$

Where, the phase factor θ is given by,

$$\theta(p_1, p_2) = 2 \tan^{-1} \left[\frac{\Delta \sin[(p_1 - p_2)/2]}{\cos[(p_1 + p_2)/2] - \Delta \cos[(p_1 - p_2)/2]} \right]. \quad (60)$$

Bound state solutions are complex and are given by the form,

$$\lambda_1 = q + i/2; \lambda_2 = q - i/2. \quad (61)$$

Here, we consider the case of infinitely long isotropic ferromagnetic chain where $\Delta = 1$ to calculate the bound

state contribution to state transfer fidelity. In this case the the number q varies continuously within the limits $-\infty < q < +\infty$. The S-matrix for bound state wave function can be calculated using the solutions given above using Equation(61),

$$\begin{aligned} e^{i\theta(\lambda_1, \lambda_2)} &= e^{2i \tan^{-1}(\lambda_1 - \lambda_2)} \\ &= e^{\log \frac{i - \lambda_1 + \lambda_2}{i + \lambda_1 - \lambda_2}} = 0. \end{aligned} \quad (62)$$

Two magnon bound state wave function apart from a normalisation factor is given by,

$$\psi_{p_1, p_2}^{x_1, x_2} = e^{i(p_1 x_1 + p_2 x_2)} \quad (63)$$

Since the momenta p_1 and p_2 are related as shown in Equation(61) the wave function for the bound state can be written in terms of the quantity q as,

$$\begin{aligned} \psi_q^{x_1, x_2} &= A(q) e^{2i[x_1 \cot^{-1}(2q+i) + x_2 \cot^{-1}(2q-i)]} \\ &= A(q) e^{x_1 \log(\frac{iq-1}{iq}) + x_2 \log(\frac{iq}{iq+1})} \\ &= A(q) \left(\frac{q^2}{1+q^2} \right)^{(x_2-x_1)/2} e^{i(x_1+x_2) \tan^{-1}(\frac{1}{q})}. \end{aligned} \quad (64)$$

Where, $A(q)$ is the normalisation factor. The normalisation factor for the wave function can be calculated as,

$$|A(q)|^{-2} = \sum_{r=1}^{N-1} r \left(\frac{q^2}{1+q^2} \right)^{N-r} \quad (65)$$

The function $G_{(B); x_1, x_2}^{x'_1, x'_2}(t)$ for an infinitely long ferromagnetic isotropic chain then becomes (using $x_{12} = x_2 + x'_2 - x_1 - x'_1$ and $\tilde{x}_{12} = x_2 - x'_2 + x_1 - x'_1$),

$$\begin{aligned} G_{(B); x_1, x_2}^{x'_1, x'_2}(t) &= \lim_{N \rightarrow \infty} \frac{N}{2\pi} \int_{-\infty}^{+\infty} \psi_q^{x_1, x_2} \psi_q^{*x'_2, x'_2} e^{-it\epsilon(q)} \frac{\partial p}{\partial q} dq \\ &= \frac{1}{2\pi} \int_{-\infty}^{+\infty} dq \frac{\partial p}{\partial q} \frac{1}{q^2} \left(\frac{q^2}{1+q^2} \right)^{x_{12}/2} e^{i\tilde{x}_{12} \tan^{-1}(1/q) - it\epsilon(q)} \end{aligned} \quad (66)$$

Where, $\epsilon(q)$ is the energy associated with the state and given in the form,

$$\epsilon(q) = \epsilon_0 + \frac{2}{1+q^2} \quad (67)$$

Two magnon scattering state wave function is given by,

$$\begin{aligned} \psi_{p_1, p_2}^{x_1, x_2} &= A(p_1, p_2) e^{i\theta(p_1, p_2)/2} \left(e^{i[p_1 x_1 + p_2 x_2 - \theta(p_1, p_2)/2]} \right. \\ &\quad \left. - e^{i[p_1 x_2 + p_2 x_1 + \theta(p_1, p_2)/2]} \right). \end{aligned} \quad (68)$$

Where, the normalisation factor $A(p_1, p_2)$ for the wave function is given by,

$$|A(p_1, p_2)|^{-2} = 4 \sum_{r=1}^{N-1} r \cos^2 \left[\frac{(N-r)(p_2 - p_1) - \theta(p_1, p_2)}{2} \right] \quad (69)$$

The function $G_{(S);x_1,x_2}^{x'_1,x'_2}(t)$ becomes,

$$G_{(S);x_1,x_2}^{x'_1,x'_2}(t) = \sum_{p_1,p_2} |A(p_1, p_2)|^2 \psi_{p_1,p_2}^{x_1,x_2} \psi_{p_1,p_2}^{*x'_1,x'_2} e^{-i\epsilon(p_1,p_2)t}. \quad (70)$$

Where, the energy eigenvalues for Heisenberg chain with anisotropy constant Δ are given by,

$$\epsilon(p_1, p_2) = \epsilon_0 + 2(\Delta - \cos p_1) + 2(\Delta - \cos p_2). \quad (71)$$

For an infinitely long chain it can be shown that the magnon momenta p_1 and p_2 become independent and

takes continuous values in an interval depending on the value of anisotropy constant Δ . For an infinitely long chain with anisotropy constant $\Delta = 1$ and Δ ($-1 < \Delta < 1$) Equation(70) becomes,

$$G_{(S);x_1,x_2}^{x'_1,x'_2}(t) = \frac{1}{4\pi^2} \int_0^{2\pi} \int_0^{2\pi} dp_1 dp_2 \psi_{p_1,p_2}^{x_1,x_2} \psi_{p_1,p_2}^{*x'_1,x'_2} e^{-i\epsilon(p_1,p_2)t}. \quad (72)$$

This can be rewritten as, using $\phi = \pi - \cos^{-1}(-\Delta)$, as

$$G_{(S);x_1,x_2}^{x'_1,x'_2}(t) = \frac{1}{4\phi^2} \int_{-\phi}^{\phi} dp_1 \int_{-\phi}^{\phi} dp_2 \psi_{p_1,p_2}^{x_1,x_2} \psi_{p_1,p_2}^{*x'_1,x'_2} e^{-i\epsilon(p_1,p_2)t}. \quad (73)$$

-
- [1] S. Bose, *Phys. Rev. Lett* **91**, 207901 (2003).
[2] V. Subrahmanyam, *Phys. Rev. A* **69**, 034304 (2004).
[3] M. Christandl, N. Datta, A. Ekert and A. J. Landahl, *Phys. Rev. Lett.* **92**, 187902 (2004).
[4] S. Sachdev, *Quantum Phase Transitions* (Cambridge University Press, Cambridge, 1999).
[5] P. Jordan and E. Wigner, *Z. Phys.* **47**, 631 (1928); E. Lieb, T. Schultz, and D. Mattis, *Ann. Phys. (N.Y.)* **16**, 406 (1961); M. Takahashi 'Thermodynamics of One-Dimensional Solvable Models' (Cambridge University Press, Cambridge, 2005).
[6] H. Bethe, *Z. Phys.*, **71**, 205 (1931).
[7] A. K. Chandra, A. Das, and B. K. Chakraborty Eds, *Quantum quenching, Annealing and Computation*. Vol. 802, Lecture Notes in Physics (Springer-Verlag, Heidelberg, 2010). , B. Sutherland, *J. Mth. Phys.* **12**, 246 (1971).
[8] M. Ganahl, E. Rabel, F. H. L. Essler, and H. G. Evertz, *Phys. Rev. Lett.* **108**, 077206 (2012).
[9] T. Fukuhara, P. Schau, M. Endres, S. Hild, M. Cheneau, I. Bloch and C. Gross, *Nature* **502**, 76 (2013); R. Vlijm, M. Ganahl, D. Fioretto, M. Brockmann, M. Haque, H. G. Evertz, and J.-S. Caux, *Phys. Rev. B* **92**, 214427 (2015).
[10] R. Steinigeweg, S. Langer, F. Heidrich-Meisner, I. P. McCulloch, and W. Brenig, *Phys. Rev. Lett.* **106**, 160602 (2011)
[11] M. S. Foster, T. C. Berkelbach, D. R. Reichman, and E. A. Yuzbashyan, *Phys. Rev. B* **84**, 085146 (2011)
[12] M. A. Cazalilla and Ming-Chiang Chung, *J. Stat. Mech.* **6**, 064002 (2016);
[13] S. R. Manmana, S. Wessel, R. M. Noack, and A. Muramatsu, *Phys. Rev. B* **79**, 155104 (2009); P. Sodano, I. A. Bayat, and S. Bose, *Phys. Rev. B* **81**, 100412 (2010); G. De Chiara, S. Montangero, P. Calabrese and R. Fazio, *J. Stat. Mech.* (2006) P03001.
[14] Lev B. Levitin and Tommaso Toffoli, *Phys. Rev. Lett* **103**, 160502 (2009).
[15] Christian K. Burrell, Jens Eisert and Tobias J. Osborne, *Phys. Rev. A* **80**, 052319.
[16] Cianciaruso, M., et al. ,*arXiv:1412.1054*. (2014).
[17] V. Subrahmanyam, and Arul Lakshminarayan. *Physics Letters A* **349.1** (2006): 164-169.
[18] Cheneau, Marc, et al. *Nature* **481.7382** (2012): 484-487.
[19] Saikat Sur and V. Subrahmanyam, *J. Phys. A* (2017)
[20] Asher Peres, *Phys. Rev. A* **30**, 4 (1984).
[21] Yu. A. Izyumov and Yu. N. Skryabin, *Statistical Mechanics of Magnetically Ordered Systems* (Springer-Verlag, Heidelberg, 1988).
[22] Man-Hong Yung *Phys. Rev. A* **74**, 030303 (2006).
[23] A. Lakshminarayan and V. Subrahmanyam, *Phys. Rev. A* **67**, 052304 (2003).
[24] R. Lima and D. Shepelyansky, *Phys. Rev. Lett.* **67**, 1377 (1991)
[25] V. Subrahmanyam, and Arul Lakshminarayan, *Physics Letters A* **349.1** (2006): 164-169.
[26] B. V Fine, T. A. Elsayed, C. M. Krodff, and A. S. de Wijn, *Phys. Rev. E* **89**, 012923 (2014).
[27] R. Jafari, and Henrik Johannesson, *Phys. Rev. Lett.* **118**, 015701 (2017).
[28] Pablo R. Zangara, Denise Bendersky, Patricia R. Levstein, and Horacio M. Pastawski, *arXiv:1508.07284* (2016).
[29] Asher Peres, *Phys. Rev. A* **30**, 4 (1984).
[30] Maksym Serbyn, Dmitry A. Abanin, *Phys. Rev. B* **96**, 014202 (2017).
[31] F. M. Cucchietti, H. M. Pastawski, and R. A. Jalabert, *Phys. Rev. B* **70**, 035311 (2004).
[32] Sunil K. Mishra and Arul Lakshminarayan, *EPL (Europhysics Letters)* **105**, 1 (2014).
[33] P. Leboeuf, J. Kurchan, M. Feingold, D. P. Arovav, *Phys. Rev. Lett* **65**, 25 (1990).
[34] Pablo R Zangara and Horacio M Pastawski, *Physica Scripta*, **92**, 033001 (2017).
[35] Juho Hoppola, Gabor B. Halasz, and Alioscia Hamma, *Phys. Rev. A* **85**, 032114 (2012).

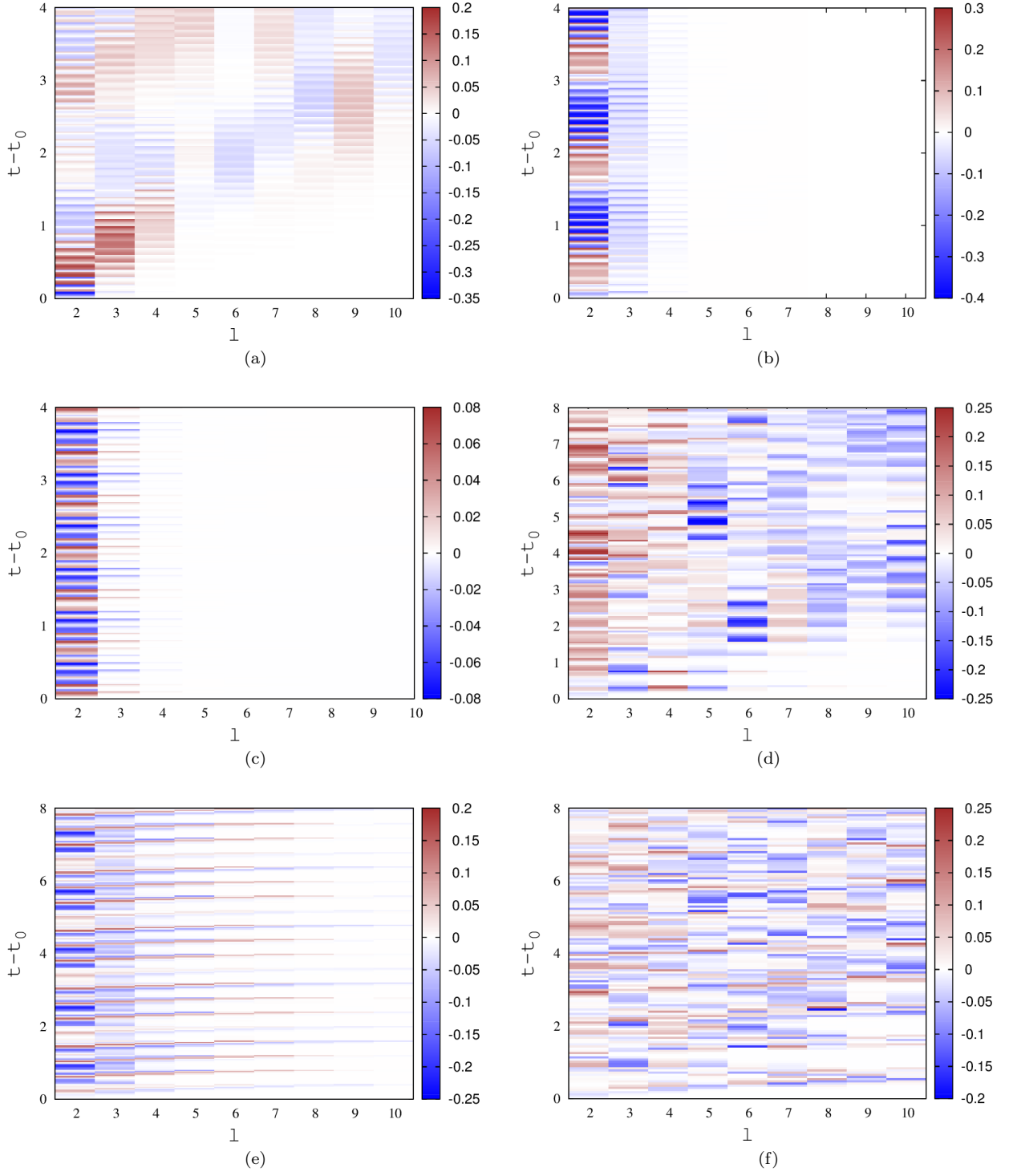


Figure 6. The detector function $f_l(t)$ as function of site index(l) and time ($t - t_0$) for kicked Harper dynamics with open boundary condition with local unitary operation on the first site after 5 kicks ($t_0 = 5\tau$) with parameters (a) $g = 1.0$ and $\tau = 0.1$, (b) $g = 3.0$ and $\tau = 0.1$, (c) $g = 10.0$ and $\tau = 0.1$, (d) $g = 1.0$ and $\tau = 0.4$, (e) $g = 2.5$ and $\tau = 0.4$, (f) $g = 1.0$ and $\tau = 0.9$. $\eta = \sqrt{2}$ for each case. The initial state in all the cases is $|\psi(0)\rangle = \sqrt{0.5}|00\dots 0\rangle + \sqrt{0.5}|100\dots 0\rangle$.